Transport in Porous Media **55:** 71–89, 2004.

Dual Mesh Method for Upscaling in Waterflood Simulation

PASCAL AUDIGANE and MARTIN J. BLUNT*
Department of Earth Science and Engineering, Imperial College, London, SW7 2AZ, U.K.

(Received: 16 October 2002; in final form: 20 June 2003)

Abstract. Detailed geological models typically contain many more cells than can be accommodated by reservoir simulation due to computer time and memory constraints. However, recovery predictions performed on a coarser upscaled mesh are inevitably less accurate than those performed on the initial fine mesh. Recent studies have shown how to use both coarse and fine mesh information during waterflooding simulations. In this paper, we present an extension of the dual mesh method (Verdière and Guérillot, 1996) which simulates water flooding injection using both the *coarse* and the original *fine* mesh information. The pressure field is first calculated on the coarse mesh. This information is used to estimate the pressure field within each coarse cell and then phase saturations are updated on the fine mesh. This method avoids the most time consuming step of reservoir simulation, namely solving for the pressure field on the fine grid. A conventional finite difference IMPES scheme is used considering a two phase fluid with gravity and vertical wells. Two upscaling methodologies are used and compared for averaging the coarse grid properties: geometric average and the pressure solve method. A series of test cases show that the method provides predictions similar to those of full fine grid simulations but using less computer time.

Key words: multiphase flow upscaling, waterflooding, IMPES scheme, reservoir simulation.

Nomenclature

D	depth.
f_j	phase fractional flow.
g	acceleration due to gravity.
G	gravity transmissivity.
$\mathbf{G}$	gravity vector.
IMPES	IMplicit Pressure Explicit Saturation scheme name.
$k_{\mathrm{r}j}$	phase relative permeability.
$k_{\mathrm{rmax}\,j}$	maximum phase relative permeability.
$\mathbf{K}$	absolute permeability tensor.
n_j	phase exponent for the Corey type relative permeability model.
P	pressure.
Q	source term.
Q_d	flux in direction d.

*Author for correspondence: Tel.: +44-20-7594-6500; Fax: +44-20-7594-7444;
e-mail: m.blunt@imperial.ac.uk

$\mathbf{Q}$	source vector.
S_j	phase saturation.
$S_{\max j}$	maximum phase saturation.
$S_{\mathrm{r}j}$	residual phase saturation.
t	time.
T	transmissivity.
$\mathbf{T}$	transmissivity matrix.
$\mathbf{v}_j$	phase velocity vector.
$\mathbf{v}_\mathrm{t}$	total velocity vector.

Greek Letters

λ_j	phase mobility.
μ_j	phase viscosity.
ρ_j	phase density.
ϕ	porosity.
∇	gradient operator.

Subscripts

g	gas.
i	fine grid block index.
j	phase index (w for water, o for oil and g for gas).
n	number total of fine grid block.
o	oil.
t	total.
w	water.

1. Introduction

Recent improvements in reservoir imaging techniques and geostatistical methods allow very detailed reservoir descriptions containing millions of gridblocks to be generated. However, time constraints in reservoir simulation generally limit the flow model to a coarser grid. Each coarse grid block property value is obtained from the original *fine* scale grid using different *upscaling* techniques.

A variety of different methods have been proposed to upscale single and multiphase flow properties. See Christie (1996), Barker and Thibeau (1997) and Barker and Dupouy (1999) for recent reviews. However, all the methods suffer from the problem that they either require a fine grid solution to derive coarse grid properties, or they make assumptions about the large scale boundary conditions that may significantly affect the results. As a consequence, despite a huge literature on multiphase upscaling, the current industry practice is to limit upscaling to single phase properties only (as an example, see Christie and Blunt, 2001). An alternative approach is to retain fine scale information while avoiding the most time consuming feature of the simulations, solving for the flow field on this fine grid. This can be achieved through solving the pressure equation at the coarse scale using appropriately upscaled properties. Heterogeneity at the fine scale can be introduced

during the saturation update by using either a pressure or a flux refinement. In this case, the precision in fluid recovery is considerably improved and the CPU time and memory are much lower than for a full fine scale simulation (Verdière and Guérillot, 1996; Gautier *et al.*, 1999).

The first implementation of a multiscale simulation technique was presented by Ramé and Killough (1991). A coarse grid finite element method was used to solve the pressure equation. Fine scale information was interpolated from the coarse grid using splines and the conservation equations for fluid transport were solved on the fine grid. 2D examples for miscible flow were presented.

Guérillot and Verdière (1995) proposed a dual mesh method where again the pressure field is first computed on a coarse grid, but where the saturation is moved on the fine grid. The velocity field is estimated within each coarse block by solving for the pressure with approximate boundary conditions. They applied this technique to a 2D single-phase model. Verdière and Guérillot (1996) extended this work to multiphase flow. They showed results in 2D for two-phase flow models with simplified injection–production boundary conditions. Comparison of the time of calculation spent for the full fine grid calculation and the dual mesh method gave a speed-up factor ranging from 5 to 7.

Guedes and Schiozer (1999) implemented the same methodology using the upscaling method of Hermitte and Guérillot (1995). They provided results in 2D including gravity effects. The well boundary conditions were considered as source or sinks applied in one grid block.

Gautier *et al.* (1999) presented a similar approach using streamline-based simulation (Batycky *et al.*, 1997). They used the pressure solve method (*psm*; Begg *et al.*, 1989) to upscale the transmissivities for each coarse grid block. They included gravity effects and wells with special attention to keep equivalent fluxes at both scales. They obtained very efficient results in terms of CPU time and memory management (speed-up factors ranging from 2 to 8 and memory saving up to 40%).

Arbogast and Bryant (2001) introduced a different dual grid approach using Green function methods to upscale transmissivities and a mixed finite element method to solve the pressure field. Gravity and capillary effects are considered in their methodology. As Gautier *et al.* (1999), they observed a reduction ratio for the time of calculation of about 2–10 compared to fine grid simulation.

Hou and Wu (1997) and Hou *et al.* (1999) derived a multiscale approach to solve the pressure equation using the finite element method. By constructing the multiscale finite element base functions that are adapted to the local property of the differential operator, this method can capture efficiently the large scale behavior of the solution without resolving the small scale features. Results are provided in 2D without gravity and capillary effects.

The objective of this paper is to extend the dual mesh method (Verdière and Guérillot, 1996) to 3D and include gravity and wells. Using the IMPES method, the pressure field is solved on the coarse mesh with a conventional finite difference scheme. Transmissivities are upscaled either with the *psm* or with a simple

geometric average (*ga*). The pressure field is reconstructed on the fine mesh using flux boundary conditions from the coarse grid simulation. The method is extensively tested and shown to perform well in a variety of circumstances. We use the SPE Comparative Solution Project (Christie and Blunt, 2001) as an example to show the limits of the method. Even though the dual mesh method technique can be inaccurate when very coarse meshes are used, it still performs better than standard coarse mesh simulation using upscaled single-phase properties.

2. Dual Mesh Method Description

In this section, we describe how the dual mesh method algorithm is implemented within the IMPES scheme. First the fluid flow equations are presented. Second, the conventional finite difference numerical scheme used for water flooding simulations is described. And finally, details on how the dual mesh method is implemented are given.

2.1. MULTIPHASE FLOW EQUATIONS

In this model, we consider immiscible and incompressible fluid displacement in a porous medium. Using Darcy law, the flow $\mathbf{v}_j$ for each phase j can be described by:

$$\mathbf{v}_j = -\frac{\mathbf{K}k_{\mathrm{r}j}}{\mu_j}(\nabla P - \rho_j \mathbf{g}), \tag{1}$$

where $\mathbf{K}$ is the absolute permeability tensor (assumed diagonal), g is the acceleration due to gravity, P the fluid pressure (no capillary pressure) and $k_{\mathrm{r}j}$, μ_j, ρ_j are respectively the relative permeability, the viscosity and the density for each phase j.

Considering the water phase, the conservation equation to solve is:

$$\phi \frac{\partial S_{\mathrm{w}}}{\partial t} + \nabla \cdot \mathbf{v}_{\mathrm{w}} = Q, \tag{2}$$

with ϕ the porosity, S_{w} the water saturation, Q a source term and t the time. $\mathbf{v}_{\mathrm{w}}$ is the sum of a viscous term and a gravity term,

$$\mathbf{v}_{\mathrm{w}} = f_{\mathrm{w}}\mathbf{v}_{\mathrm{t}} + \mathbf{K}\frac{\lambda_{\mathrm{o}}\lambda_{\mathrm{w}}}{\lambda_{\mathrm{t}}}(\rho_{\mathrm{w}} - \rho_{\mathrm{o}})\mathbf{g}. \tag{3}$$

The mobility λ_j of the phase j and the total mobility λ_{t} are defined as follow:

$$\lambda_j = \frac{k_{\mathrm{r}j}}{\mu_j}, \qquad \lambda_{\mathrm{t}} = \lambda_{\mathrm{o}} + \lambda_{\mathrm{w}}, \tag{4}$$

where the subscript w labels water and o refers to oil, and f_{w} is the water fractional flow:

$$f_{\mathrm{w}} = \frac{\lambda_{\mathrm{w}}}{\lambda_{\mathrm{t}}}. \tag{5}$$

The total velocity of the fluid $\mathbf{v}_t$ is

$$\mathbf{v}_t = \mathbf{v}_o + \mathbf{v}_w. \tag{6}$$

For each time step, the pressure field is determined with an implicit scheme using Equation (1) and provides the corresponding total velocity field $\mathbf{v}_t$. Each phase saturation is updated using an explicit scheme by solving the Equation (2) using phase velocities deduced from Equation (3) and the known total velocity.

2.2. CONVENTIONAL FINITE DIFFERENCE METHOD

The reservoir is described by n Cartesian grid blocks with a constant size Δx, Δy, Δz in the x, y, z directions, respectively. By writing the mass balance for each grid block i, connected to its six neighbors, the associated water pressure P_i can be deduced from a matrix system (Aziz and Settari, 1979):

$$\mathbf{TP} = \mathbf{G} + \mathbf{Q}, \tag{7}$$

where $\mathbf{P}$ is the vector containing the n unknown pressure values P_i for each grid block. $\mathbf{T}$ is the inter block transmissivity matrix with dimensions n^2. In a direction d ($d = x$, y or z), the inter block transmissivity $T_{d,i+(1/2)}$ between a node i and $i+1$ is the harmonic average of the block transmissivities $T_{d,i}$ in this direction. For instance, along x:

$$T_{x,i+(1/2)} = \frac{2}{1/T_{x,i} + 1/T_{x,i+1}}, \tag{8}$$

with

$$T_{x,i} = \frac{\Delta y \Delta z}{\Delta x} \lambda_{t,i} k_{x,i}. \tag{9}$$

The right hand side of (7) contains the gravity vector $\mathbf{G}$ (dimension n). Each term of this vector is a product between the difference of the depth ΔD between the considered cell and its neighbors, and the interblock gravity transmissivity $G_{d,i+(1/2)}$ which is defined for instance in x direction by:

$$G_{x,i+(1/2)} = \frac{2}{1/G_{x,i} + 1/G_{x,i+1}}, \tag{10}$$

with

$$G_{x,i} = \frac{\Delta y \Delta z}{\Delta x} \lambda_{g,i} k_{x,i}. \tag{11}$$

The total gravity mobility λ_g is:

$$\lambda_g = \left(\frac{\rho_o k_{ro}}{\mu_o} + \frac{\rho_w k_{rw}}{\mu_w} \right) g. \tag{12}$$

The term **Q** is the source term represented by the wells in the model. Each grid block perforated by a well contains a source term as defined by Peaceman (1978).

Once the initial properties of the reservoir and the boundary conditions are defined, the pressure field represented by the vector solution **P** can be determined by solving the system (7). For this, the matrix **T** needs to be inverted and this step of the simulation is the most time consuming part of the calculation. From the vector solution **P** the water velocity field is deduced and used to update the saturation using an appropriate time step constrained by the Courant–Friedrichs–Levy (CFL) conditions to ensure stable solution. Using the orientation of the corresponding phase velocity, a conventional upstream weighting technique is applied to determine the direction of the saturation update (Aziz and Settari, 1979).

2.3. THE DUAL MESH METHOD

The conventional approach in upscaling is to perform the calculations on a coarser mesh where effective transmissivities have been calculated using one of a number of different upscaling methods for multiphase flow (Christie, 1996). Both fluid pressure and the saturation are determined on the coarse mesh for each time step. This approach induces inevitably some errors in the fluid recovery since fine-scale details are lost. The dual mesh method preserves the advantages of solving the pressure field on the coarse mesh, which is less time consuming, while improving the precision of the model by re-introducing the fine mesh information during the saturation update. The dual mesh method implementation can be decomposed in five steps (see Figure 1).

2.3.1. *Step 1*

Considering one time-step in a simulation, the permeability, porosity and saturation are defined on a fine grid, as are the boundary conditions at the wells.

2.3.2. *Step 2*

In Step 2, an up-griding process has been performed on the fine mesh to produce a coarse mesh. Effective transmissivities (including multiphase effects) are computed on the coarse grid using one of a number of upscaling methods. In this work, two upscaling methods have been implemented to calculate effective transmissivities of the coarse mesh: (i) the *psm* and (ii) a *ga* of the fine cell permeabilities.

As Gautier *et al.* (1999), we used the *psm* to obtain the component of the diagonal transmissivity tensor T_d^{coarse} for each d direction ($d = x$, y or z), and the gravity transmissivity component G_z^{coarse} for each coarse grid block (as our grid geometry is Cartesian and aligned vertically, we have only one gravity transmissivity component G_z^{coarse} to estimate).

A pressure drop ΔP_d is applied along the d direction between the two faces of the coarse cell (Figure 2). No flow boundaries are applied to the other faces and gravity is ignored. The pressure field is computed and from this the exiting total

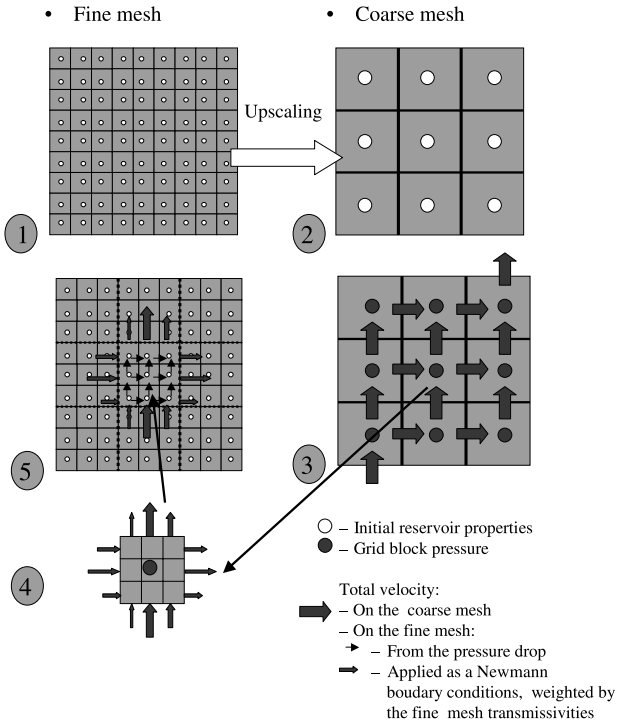

Figure 1. The dual mesh approach decomposed in five main steps. A reservoir description ① is upscaled to the coarse mesh ② using conventional methods. The pressure and total velocity are computed on the coarse mesh ③. The total velocity is used as a boundary condition to compute the pressures within each coarse block ④. The fluxes are weighted by the fine mesh transmissivities across the face. The fine-scale velocity field is used to update saturation ⑤.

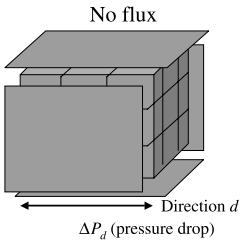

$$T_d^{\text{coarse}} = Q_d^{\text{coarse}} / \Delta P_d$$

Figure 2. The *psm* for upscaling transmissivities in each coarse grid block: in this figure the coarse grid block contains $3 \times 3 \times 3$ fine grid blocks. By applying a pressure drop ΔP_d in one direction d and no flux boundary conditions on the others, an effective transmissivity T_d^{coarse} is deduced from the calculated flow Q_d^{coarse}. A similar calculation is performed in all three directions to produce a diagonal effective transmissivity tensor.

flux of both faces Q_d^{coarse} can be calculated. The associated effective transmissivity is:

$$T_d^{\text{coarse}} = \frac{Q_d^{\text{coarse}}}{\Delta P_d}. \tag{13}$$

This is repeated for all three directions to construct a diagonal effective transmissivities tensor **T**. The transmissivity is a function both of the fine grid permeability and porosity, and the saturation distribution.

For the gravity transmissivity we do consider gravity and we apply a pressure drop equal to zero between the top and the bottom faces of the coarse grid block.

$$G_z^{\text{coarse}} = \frac{Q_z^{\text{coarse}}}{\Delta Z^{\text{coarse}}}, \tag{14}$$

with ΔZ^{coarse} the coarse grid block size in the z direction.

2.3.3. *Step 3*

Equation (7) is solved on the coarse grid to find the pressure and total velocity using the upscaled boundary conditions and transmissivities.

2.3.4. *Step 4*

From Step 3, the grid block pressure P^{coarse} and the flux Q_d^{coarse} across each face have been determined. To calculate the pressure field on the fine mesh, the following problem is solved for each coarse grid block separately. (i) The coarse fluxes are weighted by the fine mesh inter block transmissivities corresponding to the face associated to the coarse flux. Applied as a Neumann boundary condition on each coarse grid block face, the boundary condition along the x direction for the fine grid block i attached to the face f will be the flux Q_x^{fine} defined by:

$$Q_x^{\text{fine}} = \frac{T_{x,i+(1/2)}^{\text{fine}}}{\Sigma_f \; T_{x,i+(1/2)}^{\text{fine}}} Q_x^{\text{coarse}}; \tag{15}$$

and (ii) to obtain a unique solution problem the coarse pressure P^{coarse} is applied as a Dirichlet condition at the center of the coarse cell.

Using these boundary conditions and solving implicitly Equation (7), the pressures and total velocities are computed for each coarse grid block separated at the fine mesh scale.

2.3.5. *Step 5*

The total velocity computed in Step 4 is an approximation to the true solution, but its normal component is everywhere continuous across cell faces, so that in the saturation update, mass is conserved exactly. If the fine grid block does not have any face connected to the next coarse grid block, the velocity is found from the pressure gradient between its neighbors (this corresponds to the thin arrow in Figure 1 Step 5). If the fine grid block has a face connected to the next coarse grid

block, the flux boundary condition Equation (15) is used to define the total velocity (thick arrow in Figure 1 Step 5).

Hence, at the end of the Step 4, the total velocity field is found on the whole initial fine mesh, so that the saturation field can be updated using standard single-point upstream weighting (Aziz and Settari, 1979).

3. Test Cases

In this section, different cases are presented to test the dual mesh approach. For each case, four simulations will be run. The first simulation corresponds to a conventional run performed on the fine mesh. This will correspond to the *fine* model in the following. The second model is the one performed on the coarse mesh only (*coarse* case in the following), which means that the absolute permeability is upscaled with simple *ga*. Saturation is updated on the coarse mesh. This corresponds to a standard approach to upscaling. The third and fourth cases correspond to the use of the dual mesh approach previously described using two different techniques to upscale transmissivity: the *psm* and *ga*.

3.1. 2D HORIZONTAL

The first example showed in this study corresponds to a 2D case with a fine mesh composed of 30 by 30 cells and a coarse mesh of 10 by 10 cells (Figure 3). The permeability field is a distribution of two facies representing high (in white) and a low (in black) values, 100 and 1 mD, respectively. The proportion of the black facies is 20%. The porosity is constant and equal to 0.25. Water is injected at one corner of the grid at a rate of 5 m^3/day, and the fluid is produced at a constant pressure equal to 76 bars at the opposite corner. The relative permeability model

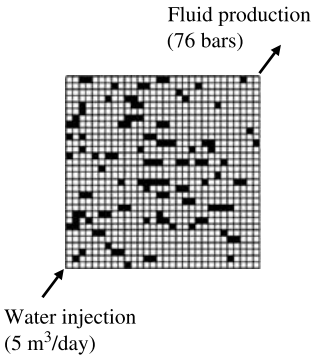

Figure 3. The 2D horizontal case corresponds to 30 × 30 cells for the fine mesh and 10 × 10 for the coarse mesh. The permeability field is distributed with high permeable zones at 100 mD (in white) and low permeable zones at 1 mD (in black). The porosity is constant at 0.25 and injection and production zones correspond to the two opposite corners of the grid. The reservoir size is 300 m by 300 m by 1 m.

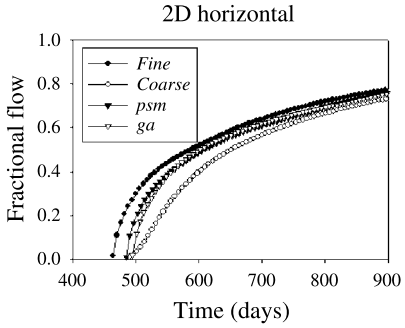

Figure 4. Watercut comparison, for the 2D horizontal case, between simulations performed on the initial fine mesh (*fine*), the coarse mesh (*coarse*), and the dual mesh method using *ga* and *psm* for upscaling.

used for all the test cases is the conventional Corey-type function:

$$k_{rj}(S_j) = k_{rmaxj}\left(\frac{S_j - S_{rj}}{S_{maxj} - S_{rj}}\right)^{n_j}, \tag{16}$$

with $k_{rmaxo} = 1$, $k_{rmaxw} = 0.4$, $S_{maxo} = S_{maxw} = 0.8$, $S_{ro} = S_{rw} = 0.2$, $n_w = 1.5$ and $n_o = 2$. The oil viscosity is 0.8 cP and the water viscosity is 1 cP.

Figure 4 shows the watercut or fractional flow (the volume fraction of the total flow out of the well that is water) at the production well for the four different models (*fine*, *coarse*, *psm* and *ga*). The difference between the *coarse* and the *fine* simulated watercut is quite significant. The dual mesh approach improves considerably the watercut estimate especially for the *psm* model. The simulation performed for the *ga* model corresponds approximately to the test performed by Verdière and Guérillot (1996) and provides similar results for the simulated watercut.

Figure 5 shows a comparison of the saturation field for each simulations after 300 days of injection. Once again, one can see clearly how well the dual mesh method is able to restore the fine mesh heterogeneity during the water injection simulation compared with the average front described by the coarse model.

3.2. 3D IMPLEMENTATION

Considering the vertical direction implies the addition of two more steps in the simulation process: first, the gravity segregation term in the saturation update, and second, the well boundary conditions.

3.2.1. *Gravity Segregation*

During the saturation update, described by the Equation (2), the difference of phase densities induces a vertical displacement defined by the second term of the Equation (3). This vertical displacement has to be considered for a model containing

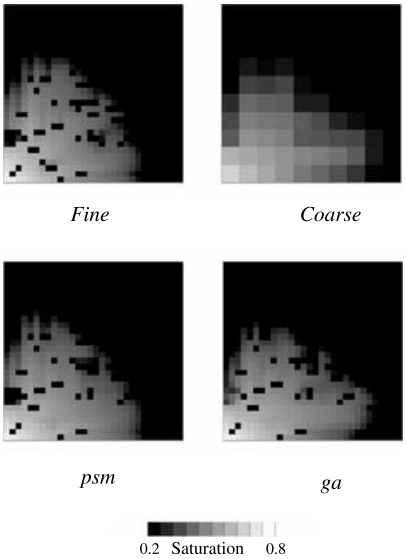

Figure 5. Comparison of the saturation field simulated after 300 days of injection for the fine mesh (*fine*), the coarse mesh (*coarse*) and the dual mesh method with the *psm* and *ga*.

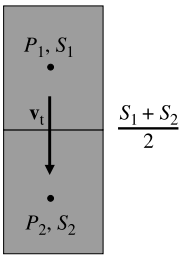

Figure 6. To determine an upstream direction for each phase at a grid face, phase mobilities are calculated using the average saturation of the two adjoining grid blocks. Then Equation (3) is used to determine the sign of $\mathbf{v}_w$. This determines the upstream direction.

more than one layer in the vertical direction. The traditional manner to perform this step with the IMPES scheme is to determine the upstreaming direction defined by each phase velocity by considering the pressure gradient between two adjacent grid blocks (Eq. (1)). However, as mentioned in Section 2.3.4, to respect mass balance the normal component of the total velocity is continuous while the pressure will be discontinuous across the coarse cell faces, resulting in an erroneous determination of the upstream direction in some cases.

To apply single-point upstream weighting we need to define an upstream direction for the water velocity at each fine cell face. With gravity effects the direction is not necessary the same as the total velocity. Consider two blocks 1 and 2 connected by a face (Figure 6). We compute mobilities using an average saturation $S_{av} = (1/2)(S_1 + S_2)$. These mobilities are used in Equation (3) to determine the sign of $\mathbf{v}_w$ and hence the appropriate upstream direction. Once the upstream

direction is known, the phase mobilities used for the saturation update are functions of the saturation of the upstream grid block.

3.2.2. *Well Boundary Conditions*

The wells are treated exactly the same as in Gautier *et al.* (1999). For each fine grid block i perforated by a well, we define the source term $Q^{\text{fine}}_{i,\text{well}}$ due to the well at the fine scale by:

$$Q^{\text{fine}}_{i,\text{well}} = \frac{T_{i,\text{well}}}{\Sigma^{\text{well}}_i T_{i,\text{well}}} Q^{\text{coarse}}_{\text{well}}, \tag{17}$$

where $T_{i,\text{well}}$ is the well transmissivity defined by Peaceman (1978) and $Q^{\text{coarse}}_{\text{well}}$ is the coarse scale well flux of the associated coarse grid block. Hence, the coarse scale source term is redistributed at the fine scale taking into account the fine mesh heterogeneity.

3.2.3. *2D Vertical Example*

The first example with gravity is a 2D case oriented along the vertical direction (Figure 7(a)). Once again a two facies permeability model has been generated with one permeability value at 100 mD (in white) and 0.1 mD (in black). The fine mesh is a 60 by 60 grid while the coarse mesh is 10 by 10. The reservoir size is 900 m by 600 m by 60 m in the x, y and z directions, respectively. Water is injected on the left side with a constant rate equal to 100 m^3/day and the fluid is produced on the right side of the model with a constant bottom hole pressure of 80 bars. In order to quantify the gravity effects in this study we use the same gravity number N_{g} used by Gautier *et al.* (1999):

$$N_{\text{g}} = \frac{\Delta\rho g L^2}{\Delta P_h H}, \tag{18}$$

which represents the ratio between viscous and gravity forces. $\Delta\rho$ defines the difference in density between water and oil, ΔP_h and L are the pressure difference and distance between the two wells and H is the height of the reservoir. In this simulation the gravity number is equal to 0.3, typical of reservoir displacements.

Figure 8 presents the watercut simulated for the four different approaches. The dual mesh approach using the *psm* is virtually identical to the fine grid and much more accurate than using the *ga*. The saturation fields (Figure 7(b)) show that once again the dual mesh method captures the heterogeneity defined by the permeability on the fine mesh.

3.3. 3D RESULTS

In order to study the performance of the dual mesh method for more complex cases, three different scenarios have been generated using an upscaled version of the SPE

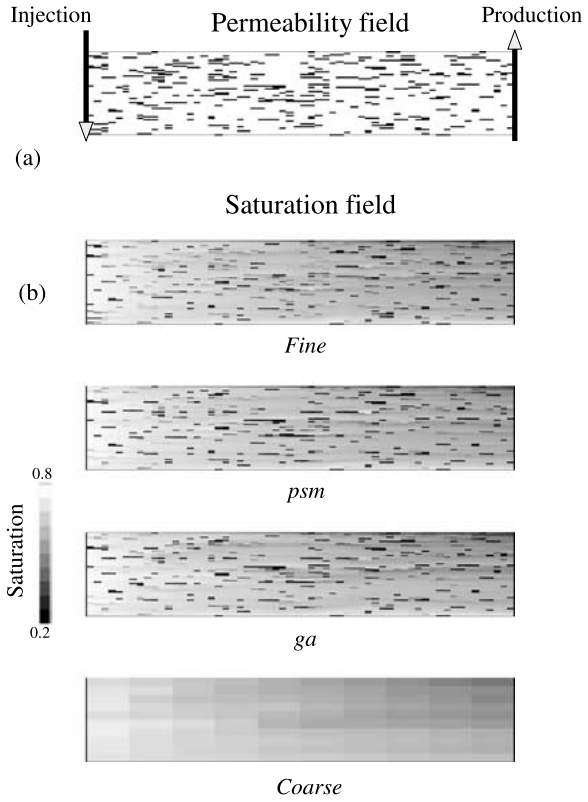

Figure 7. (a) Permeability field for a 2D case with gravity effects. Two facies are simulated: 0.1 mD in black and 100 mD in white. (b) Comparison of the saturation field simulated after 1000 days of injection for the fine mesh (*fine*), the coarse mesh (*coarse*) and the dual mesh method with the *psm* and the *ga*.

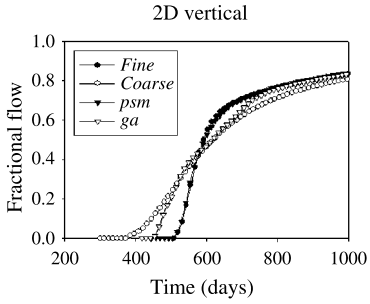

Figure 8. Watercut comparison, for the 2D vertical case, between simulations performed on the initial fine mesh (*fine*), the coarse mesh (*coarse*), and the dual mesh method using *ga* and *psm* for upscaling.

Comparative Project on upscaling (Christie and Blunt, 2001). The original grid has been upscaled in order to be able to run the fine mesh simulation (the original fine mesh contains approximately one million grid blocks). To compare results from

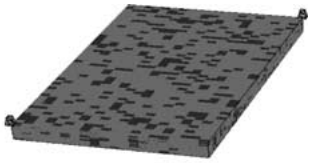

(a) Scenario 1

(b) Scenario 2

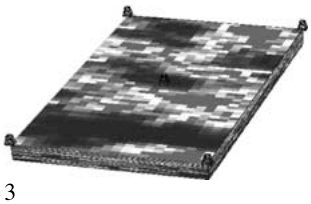

(c) Scenario 3

Figure 9. Three different scenarios for the permeability and porosity fields used for testing the dual mesh method: (a) constant porosity at 0.2 with a dual facies permeability (100 mD in grey and 1 mD in black) and one injector and one producer well, (b) same as (a) but with one injector and four producers, (c) an upscaled version of the SPE Comparative Project 2001 (Christie and Blunt, 2001) with one central injector and four producers.

the same source code the dimension of the problem has been reduced to a grid with 93,500 cells ($20 \times 55 \times 85$).

The three test cases are shown in Figure 9. For Scenario 1, the porosity is constant and equal to 0.2 and the permeability is governed by a dual facies model with 80% at 100 mD and 20% at 1 mD. The water is injected at one corner and the fluid is produced at the opposite corner. For Scenario 2 the heterogeneity is exactly the same as the first scenario but the well completion consists in one central injector and four producers at each corner of the reservoir grid. For Scenario 3, the well completion is the same as Scenario 2 but the permeability and the porosity corresponds to an upscaled version of the SPE Comparative Project 2001. The permeability is upscaled using *ga*. The top part of the model is a Tarbert formation, and it is a representation of a prograding near shore environment while the lower part (Upper Ness) is fluvial.

All the wells are vertical and completed throughout the whole formation. The water is injected at 795 m^3/day while the fluid is produced with a constant bottom hole pressure at 275 bars. The fine mesh contains 20 by 55 by 85 cells (93,500 gridblocks) while the coarse mesh is a 5 by 11 by 5 cells (275 gridblocks). Each fine cell is a 6.096 m by 3.048 m by 0.6096 m Cartesian grid block. The Corey-type

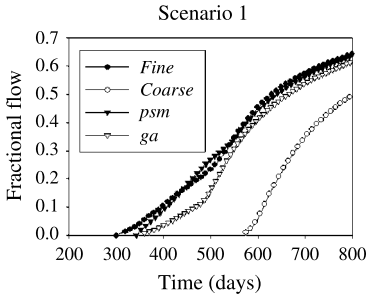

Figure 10. Watercut comparison for Scenario 1 between simulations performed on the initial fine mesh (*fine*), the coarse mesh (*coarse*), and the dual mesh method using *ga* and *psm* for upscaling.

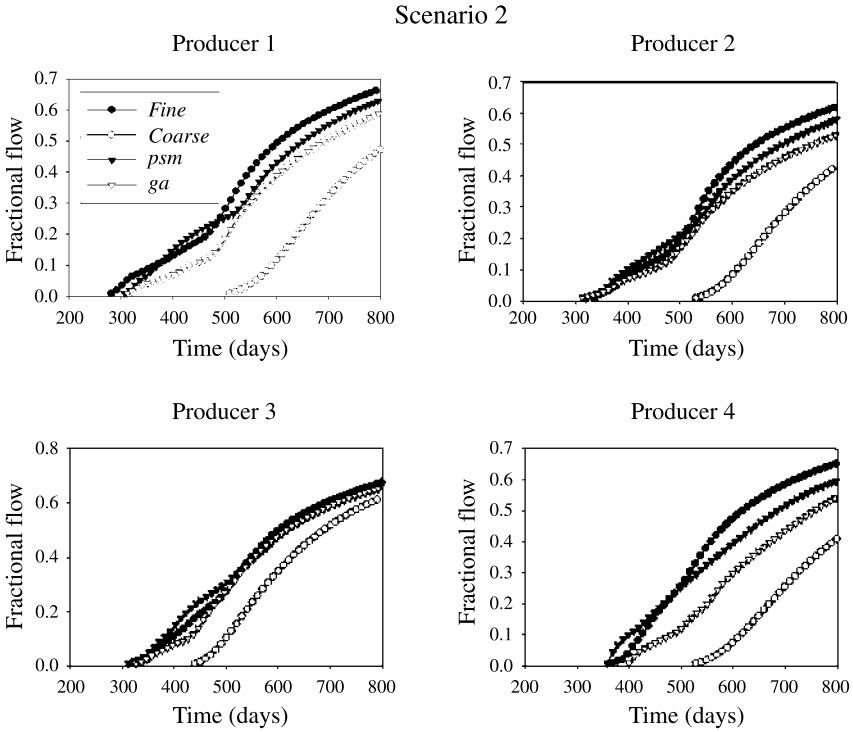

Figure 11. Watercut comparisons, for each producer, for Scenario 2 between simulations performed on the initial fine mesh (*fine*), the coarse mesh (*coarse*), and the dual mesh method using *ga* and *psm* for upscaling.

relative permeability functions have been used with $n_o = n_w = 2$, $k_{rw} = k_{ro} = 0.2$ and $k_{rmaxo} = k_{rmaxw} = 1$. Densities for oil and water are respectively 850 and 1000 kg m^{-3} and viscosities are 3.0 cP for oil and 0.3 cP for the water.

For Scenario 1, Figure 10 shows that the dual mesh method is able to reproduce the fine grid watercut much better than the simulation on the coarse mesh. The use

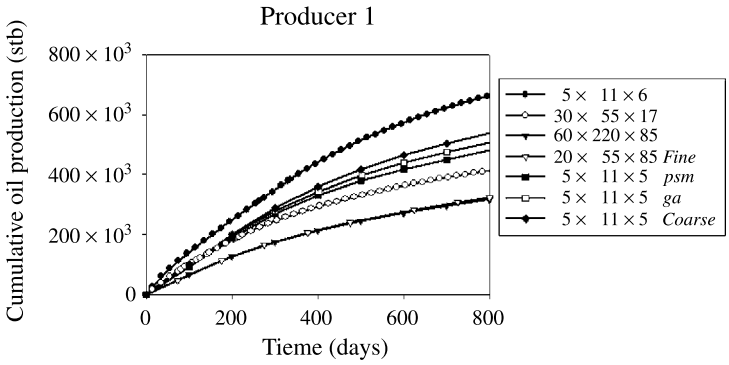

Figure 12. Cumulative oil production comparison for producer 1 in Scenario 3 with different grid sizes using the single phase upscaling *psm* (by Christie and Blunt, 2001). Our *fine* case ($20 \times 55 \times 85$) is close to the initial fine mesh ($60 \times 220 \times 85$). The results are compared to our coarse case ($5 \times 11 \times 5$, using geometric averaging) and the dual mesh method with *ga* or the *psm*.

of the *psm* improves considerably the precision of the result in comparison with a simple *ga*.

By increasing the number of wells (Scenario 2), the same trend is observed for each producer (Figure 11): between the *psm*, the *ga* and the *coarse* case the *psm* is the closest to the *fine* simulation.

Scenario 3 is rather different (Figures 12 and 13), and the dual mesh method does not perform better than the coarse grid simulation in all cases. For producers 3 and 4 the *psm* is closer to the *fine* model compared with the two others, especially for well 4. On the other hand, for well 1 and 2 the *psm* model gives worse results than the *coarse* model which is not the case for the *ga* model. In this case the *ga* model always gives better estimates than the *coarse* one.

In Figure 12, the cumulative oil production for producer 1 is compared with results using single-phase upscaling by the *psm* presented by Christie and Blunt (2001). The *fine* case ($20 \times 55 \times 85$), which corresponds to our fine mesh simulation, is close to the original fine mesh simulation ($60 \times 220 \times 85$) performed by Christie and Blunt (2001). This case is chosen to demonstrate where upscaling methods break down. When the upscaled grid is exceptionally coarse, single-phase upscaling using the *psm* ($5 \times 11 \times 6$) gives a very poor prediction of recovery for some wells – typically when the production rate from the well is low. Using geometric averaging for single phase upscaling on a $5 \times 11 \times 5$ mesh (*coarse* results) is an improvement but is still far from the fine scale results. The dual mesh method (*psm* and *ga*) performs only slightly better. However, note that in Figure 13 the dual mesh method results for producer 1 are worse in predicting watercut than the coarse grid, while they are better at predicting cumulative production. The reason for this is that the dual mesh method better captures the total mobility of the system.

The accuracy of the dual mesh method depends on the complexity of the reservoir heterogeneity. In Scenarios 1 and 2 the high percentage of high permeable

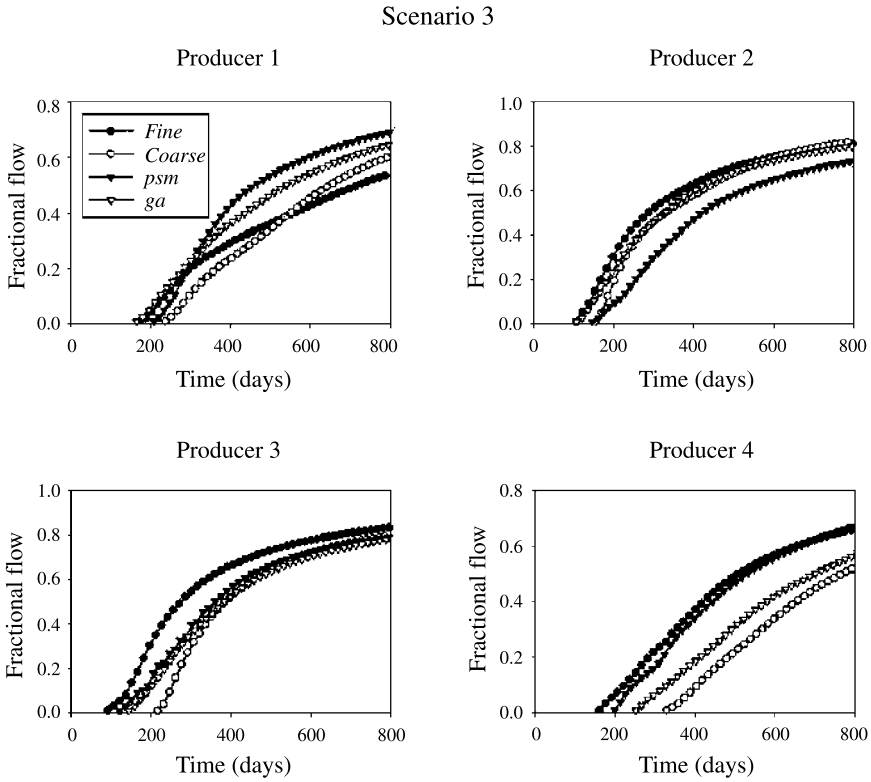

Figure 13. Watercut comparison, for each producer, for Scenario 3 (upscaled version of the SPE Comparative Project 2001) between the simulations performed on the initial fine mesh (*fine*), the coarse mesh (*coarse*), and the simulations performed using the dual mesh method with either *ga* or the *psm* for upscaling the properties.

facies (80%) is easier to upscale with the *ga* and *psm* upscaling techniques than the channeling pattern of the reservoir in Scenario 3. From the watercut comparison, Scenario 3 (Figure 13) shows that the dual mesh method using a *ga* (*ga* model) matches quite well the *fine* model for early times, but it seems to converge to the *coarse* model at late times.

4. Discussion and Conclusions

The dual mesh method is generally faster than the fine grid simulation. A speed-up factor is defined as the ratio between the time needed to perform the simulation on the *fine* mesh and the time needed for the studied case (*ga*, *psm* and *coarse*). This has been calculated for each model in Table I. The speed-up factor is dependent on the complexity of the problem. If the *fine* simulation can be quickly run, the dual mesh method can be even slower (case 2Dh). But there is no sense in upscaling such a small model. The speed-up factor increases to a value around 4 for Scenario 3,

Table I. Speed factor comparison. The 2Dh, 2Dv models correspond to the 2D test cases, horizontal and vertical respectively, presented in the Sections 3.1 and 3.2.3. Scenario 3 is the upscaled version of the SPE Comparative Project 2001

Model	2Dh	2Dv	Scenario 3
Fine mesh	30×30	60×60	$20 \times 55 \times 85$
Coarse mesh	10×10	10×10	$5 \times 11 \times 5$
ga	0.9	2.1	3.9
psm	0.6	1.3	3.1
coarse	3.6	28	432

which corresponds to the most complex problem treated in this study. This value corresponds approximately to those estimated by Gautier *et al.* (1999) and Verdière and Guérillot (1996). However, as discussed by Arbogast and Bryant (2001) the speed of the upscaling method is difficult to quantify as it depends on multiple factors (mesh, solved equations, code efficiency). In their case, they estimated a range 2–10 for a standard cell-centered finite difference scheme.

This paper has extended the dual mesh method to 3D cases with gravity incorporating a proper treatment of wells. In terms of oil recovery, this method does perform better than the other methods for all cases studied, and does considerably better than standard single-phase upscaling. On the other hand, it can perform poorly in terms of watercut prediction (Scenario 3). This means that the method correctly captures the total mobility of the system. The method becomes worse as the mesh is made coarser and for increasingly heterogeneous systems. However the method works well for a variety of test cases with a saving in computer time compared to fine scale simulation.

Acknowledgements

The authors are grateful to the EPSRC, DTI and the sponsors of the Imperial College Consortium on Pore Scale Modeling (BHP, Shell, Enterprise, Statoil, PDVSA-Intervep, Schlumberger, Gaz de France and JNOC) for financial support.

References

Arbogast, T. and Bryant, S. L.: 2001, Numerical subgrid upscaling for waterflood simulations, *SPE Reservoir Simulation Symposium*, SPE No. 66375, Houston, 11–14 February.

Aziz, K. and Settari, A.: 1979, *Petroleum Reservoir Simulation*, Applied Science, London.

Barker, J. W. and Dupouy, Ph.: 1999, An analysis of dynamic pseudo relative permeability methods, *Petroleum Geoscience* **5**, 385–394.

Barker, J. W. and Thibeau, S.: 1997, A critical review of the use of pseudo relative permeabilities for upscaling, *SPE Reservoir Engineering May* **12**, 138–143.

Batycky, R. P., Blunt, M. J. and Thiele, M. R.: 1997, A 3D field-scale streamline-based reservoir simulator, *SPE Reservoir Engineering* **11**, 246–254.

Begg, S. H., Carter, R. R. and Dranfield, P.: 1989, Assigning effective values to simulator gridblocks parameters for heterogeneous reservoirs, *SPE Reservoir Engineering* **4**, 455–464.

Christie, M. A.: 1996, Upscaling for reservoir simulation, *JPT* **48**, 1004–1008.

Christie, M. A. and Blunt, M. J.: 2001, Tenth SPE Comparative Solution Project: comparison of upscaling techniques, *SPE Reservoir Engineering and Evaluation August* **4**, 308–317.

Gautier, Y., Blunt, M. J. and Christie, M. A.: 1999, Nested griding and streamline-based simulation for fast reservoir performance prediction, *Computational Geosciences* **3**, 295–320.

Guedes, S. S. and Schiozer, D. J.: 1999, An implicit treatment of upscaling in numerical reservoir simulation, *SPE Symposium on Reservoir Simulation*, SPE 51937, Houston, 14–17 February.

Guérillot, D. and Verdière, S.: 1995, Different pressure grids for reservoir simulation in heterogeneous reservoirs, *SPE Symposium on Reservoir Simulation*, SPE No. 29148, San-Antonio, 12–15 February.

Hermitte, T. and Guérillot, D.: 1995, A more accurate numerical scheme for locally refined meshes in heterogeneous reservoirs, *SPE Symposium on Reservoir Simulation*, SPE No. 25261, New Orleans, 28 February–3 March.

Hou, T. Y. and Wu, X. H.: 1997, A multiscale finite element method for elliptic problems in composite materials and porous media, *Journal of Computational Physics* **134**, 169–189.

Hou, T. Y., Wu, X. H. and Cai, X.: 1999, Convergence of a multiscale finite element method for elliptic problems with rapidly oscillating coefficients, *Mathematics of Computation* **227**, 913–943.

Kyte, J. R. and Berry, D. W.: 1975, New pseudo functions to control numerical dispersion, *SPEJ* **15**, 269–275.

Peaceman, D. W.: 1978, Interpretation of well-block pressures in numerical reservoir simulation, *SPEJ* **18**, 183–194.

Peaceman, D. W.: 1997, Effective transmibilities of a gridblock by upscaling-comparison of direct methods with renormalisation, *SPEJ* **2**, 338–349.

Ramé, M. and Killough, J. E.: 1991, A new approach to the simulation of flows in highly heterogeneous porous media, *SPE Symposium on Reservoir Simulation*, SPE No. 21247, Anaheim California, 11–17 February.

Renard, P. and de Marsily, G.: 1997, Calculating equivalent permeability: a review, *Advances in Water Resources* **20**, 253–278.

Verdière, S. and Guérillot, D.: 1996, Dual mesh method for multiphase flows in heterogeneous media, *5th European Conference on the Mathematics of Oil Recovery*, Leoben, Austria, 3–6 September.